

Cavity Vertex Regeneration through Optimal Energy Model for Restoration of Worn Parts

Jian Gao*, Xiangping Zeng, Xu Zhang, Xin Chen, and Detao Zheng

School of Electromechanical Engineering, Guangdong University of Technology,
Key Laboratory of Mechanical Equipment Manufacturing & Control Technology, Ministry of Education,
Guangzhou, 510006, China

*Corresponding author, e-mail: gaojian@gdut.edu.cn

Abstract

Restoration of worn parts is a key technique in remanufacturing engineering. It is also a popular research topic in the domain of sustainable manufacturing. To tackle the difficult problem of obtaining a reference model for repair of worn parts, this paper proposed a novel approach to regenerate the vertices over the worn cavity. After a brief description of the repair process, this paper focuses on the optimal energy model establishment. Based on the energy model the vertices of the worn cavity can be regenerated. Error calculation of the vertices recreated to the original model is proposed to search the shortest distance. These algorithms proposed were implemented in the repair system through Visual C++6.0. Several examples of worn parts are presented to illustrate the feasibility of the method. The testing result shows that the vertex regenerated through the optimal energy model can satisfy the requirement of accurate geometry regeneration for repair of worn parts. Finally, conclusions are drawn and further research work is discussed.

Keywords: Remanufacturing, Energy Model, Vertex Regeneration, Part Repair

Copyright © 2013 Universitas Ahmad Dahlan. All rights reserved.

1. Introduction

Presently more and more industrial sectors have a growing interest in refurbishment of worn parts and reusing of them. These industries include aerospace, power generation, die and mould, historical object restoration industries, and so on. Refurbishment of worn parts means to repair and remanufacture the damaged parts or objects and to extend their life cycles. It is therefore a significant research direction to support the development of global sustainable manufacturing. To avoid endless repetition the authors use the word "worn", but the reader may assume worn, damaged or any other form of defect, except deformation caused by the overall twisting of the surface.

In the repair process, the most difficult problem is lack of a reference geometrical model (a CAD model) for the worn objects. In most cases, the CAD models for the worn parts may not be used because: 1) variations in the manufacturing process make each component geometrically unique, in addition, severe wear of the parts in service makes the original CAD model no longer representative of the geometry of the worn parts [1, 2]. 2) use of the original CAD models is prohibited due to proprietary reasons [3]. 3) the original CAD models are lost after years in service. In order to precisely refurbish and repair parts such as expensive aero-components, die and mould parts or valuable antiques, reconstruction of surface reference model for the damaged object is a key issue for the success of refurbishment of used parts in various applications.

In this paper, we describe a complete repair system which includes processes of boundary identification, facet deletion, vertex regeneration and surface reconstruction to the existing damaged objects. New techniques for solving the key problems, such as adjacent data extraction and optimal energy model based vertex regeneration of the worn cavity, have been proposed and implemented in the system. Cavity vertex regeneration is used to recreate vertices over the worn cavity based on the control points of the undamaged adjacent areas of the digitised parts, which can preserve the shape of the undamaged model. Several examples are presented to demonstrate the feasibility of the proposed approach.

The remainder of this paper is organized as follows: Section 2 presents a discussion of the related work in the literature. Section 3 gives a brief description of the repair process for damaged parts. In Section 4, we present the vertex regeneration method for the worn cavity through the algorithm of optimal energy model. Error evaluation for the cavity vertex is performed in Section 5. In Section 6, we demonstrate several examples to verify the proposed method. Section 7 presents conclusions and directions for future research possibilities.

2. Related Work

As the increasing awareness of environment and limited natural resources, more manufacturers have been considering how to refurbish and repair large quantities of worn components, causing more researchers to focus their efforts on the development of more sustainable manufacturing methods. These worn parts are either too expensive to dispose of in a responsible manner or too valuable to replace. Currently, a number of industries have reported successful applications of their remanufacturing strategy, for example, aeroengine components [4-6], expensive die and mould parts [7], historic antiques [8]. Due to various defects of the worn objects such as deformation, wear, chips and cracks, it is impossible to remanufacture these parts without reconstructing a model representing and adapted to the geometry of the used part [2]. In case of an antique restoration, Huang [8] presents a complete recovery of a broken ceramic vase without a CAD model or any technical drawings through a Many-Knot spline interpolation algorithm. Bagci [3] proposed a Reverse Engineering (RE) technique to reproduce the CAD models of the worn parts. Through the step-by-step recovery procedure, surface models of three exemplified parts including a turbine blade, bust figurine and a human head are reconstructed and their surface continuity is analysed by the iso-photo method. Gao and Chen [9] presents a RE-based approach to reconstruct a nominal surface model adapted to the blade geometry to be repaired.

In an RE system, the main problem is the restoration of missing data, such as holes in the digitised model caused by imperfect data capture, or surface reflectance, occlusions and accessibility limitations. Holes must be filled and closed to form a continuous “watertight” polygonal model for successful RE processes. Considering the research work for filling holes and reconstructing surface models, there are a number of papers available. Techniques to solve the problem fall into several categories: interpolating and fitting reconstruction [10, 11], Delaunay-based Surface Reconstruction [12, 13], deformed reconstruction [14, 15], neural network based reconstruction [16, 17], and Support Vector Machine (SVM) based reconstruction [18, 19]. Owing to the structure risk minimization theory, SVM method is shown in [18] to be a better way to overcome the disadvantages of a neural network based method such as local optimization, lack of generalization, etc. Chui et al. [20] used the method of energy minimization to fill polygonal holes. Curless and Levoy [21] proposed a method to interpolate non-sampled surfaces in concave regions of volumetric parts. They produced watertight models using a volumetric method of filling holes in voxel space for reproduction using rapid prototyping techniques. Liepa [22] described a method for filling holes in unstructured triangular meshes. The resulting patch interpolates the shape and density of the surrounding mesh. In order to overcome the problems associated with existing methods, limited to small holes and smooth area, Jun [23] proposed an automated algorithm that fills complex holes. This method identifies the polygonal holes in a 3D triangular mesh and consecutively fills them regardless of the shape complexity of the holes. The algorithm first divides a complex hole into several simple sub-holes incrementally with respect to the complexity of the hole. Then all the sub-holes are sequentially filled with the planar triangulation until the whole complex hole is firmly closed. Smoothing and subdivision modules are then applied to the new mesh triangles covering the hole to refine the shape quality by comparing them to the existing neighbor triangles. The newly created vertices and triangles are added to their respective lists and the topology information is updated. Wang and Oliveira [24] present an algorithm to fill holes on smooth surfaces reconstructed from point clouds. The algorithm is based on moving least squares and can interpolate both geometry and shading information. The approach can fill holes in both manifold hole and create surfaces with boundaries. In the case of surfaces with boundaries, user assistance is required to resolve the inherent ambiguity associated with surface reconstruction.

As we all know, the majority of RE applications have focused on surface reconstruction to suit CAD/CAM systems for the purpose of product design, replica, manufacture or inspection

[1, 25-29]. For the use of repairing and remanufacturing of damaged parts, especially regenerating the original geometry of worn-out area, the RE-based reconstruction method contains too many manual operations in creating the surface model. Therefore it is difficult to guarantee a stable modeling environment or to automate the process, and it is not an appropriate tool for the automatic repair of large numbers of worn objects in industry.

In this paper, we propose a novel algorithm to regenerate the missing vertices over the worn area which can be used to create a surface model for tool path generation of repair process, including building up the missing area and machining away the unwanted material. Based on the adjacent available data, the kernel of the proposed algorithm is to regenerate vertex of the worn cavity through an optimal energy model. Error evaluation is performed to evaluate accuracy of the regenerated points over the worn cavity to the original surface model. Case study is performed and several worn parts are exemplified to validate the proposed method.

3. Repair Process Description

A digitised model needs to be created by a digitisation system for the objects being repaired. Currently, most digitisation systems can provide the part's cloud points with a fast scanning speed and high density, and integrate each scan automatically into a 3D model. The output model is in a format of polygonal STL (Sterolithgraphy) file. Using this surface model, the repair process implements three procedures: 1) identify worn area, determine worn boundary and delete the mesh within the boundary; 2) obtain the control points from adjacent un-worn area and regenerate the vertices over the worn area; 3) reconstruct the surface model based on the regenerated points. This "repaired" surface model provides the geometry for planning the repair tool paths of the build-up and machining processes. Fig.1 illustrates the main procedures of the repair process.

In general, a worn part needs to go through several refurbishing procedures before it can be satisfactorily returned to service: 1) digital model acquisition; 2) worn boundary identification and extraction; 3) data point and surface regeneration over the worn cavity; 4) tool paths generation for the build-up and machining process. Figure 1 shows the main procedures involved in the repair system. In this system, the 3D geometry of the worn part to be repaired is digitised through a non-contact scanner and a polygonal model is created and used in the repair system. Obviously, the mesh of the worn areas does not represent the original geometry of the part and they need to be identified, eliminated and regenerated. Based on the method proposed in our previous paper [30], the boundary of worn area can be extracted and the mesh within the worn boundary can be deleted automatically. This paper focuses on how to regenerate the vertices over the worn cavity based on the undamaged vicinity of the hole.

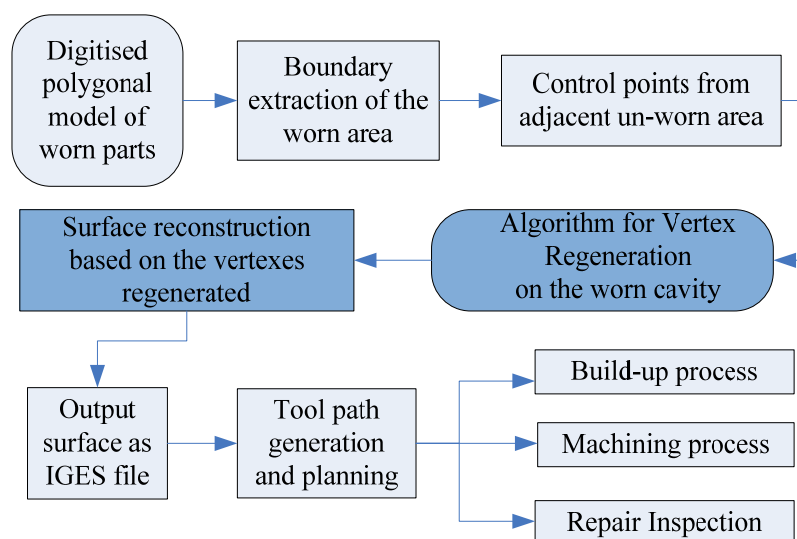


Figure 1. System structure for the refurbishment of worn parts

4. 4. Optimal Energy Model Based Cavity Vertex Regeneration

4.1. Adjacent Data Extraction

A polygonal model comprises a set of triangle facets to approximately represent the surface geometry of the part. Each one of the facets is represented through 3 vertices and one facet normal. For a worn object, the defects can be detected on the scanned polygonal model by the curvature change of the worn area, by comparing the angle between the normal for adjacent facets.

In this paper, we define the angle between the normal of two adjacent facets as Facet angle (F-angle) shown in Figure 2 and the threshold of the F-angle can be set in advance and revised according to different model. When the calculated angle is larger than the value, then the common edge of the two facets is part of the boundary of the worn area, and the two points of the edge are called the boundary vertices. Once the boundary is identified and extracted through the F-angle, the facets within the worn area can be deleted since these facets do not represent the original geometry of the worn part. The details about boundary extraction and facets deletion can refer to our previous paper [30]. Based on the cavity boundary, the adjacent data on the undamaged vicinity can be obtained, which is shown in Figure 3.

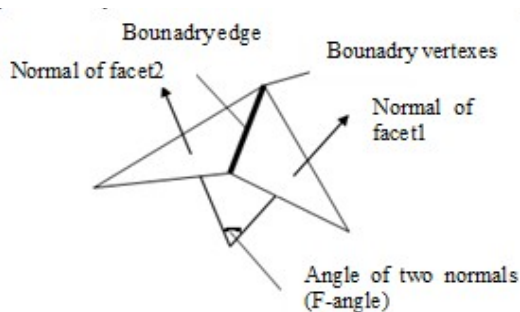


Figure 2. Facet angle

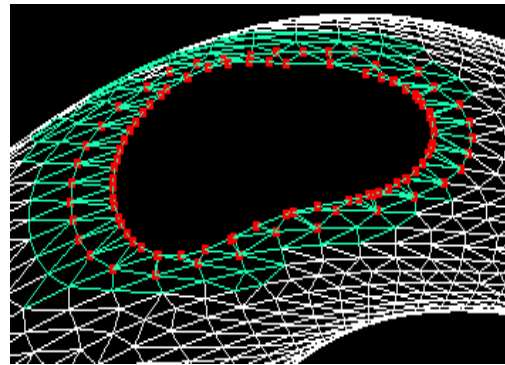


Figure 3. Adjacent data extracted

4.2. Energy Model

The kernel idea of the optimal energy modeling is that it is a modeling method aiming at minimizing the deformation energy possessed by curve and surface, controlling the shape of curve and surface through various constraints and applied loads. In other words, the optimal energy modeling is to find the curve and surface with minimized physical deforming energy under the conditions of geometric and non-geometric constraints.

Therefore, the first step of the optimal energy modeling is to establish the optimal function, and determine the meaning of physical deforming energy. In general, physical deforming energy can be expressed by the elastic deforming equation of thin plane, which has the representation of:

$$E_{curve} = \int (\alpha W_u^2 + \beta W_{uu}^2 - 2fw) d_u \quad (1)$$

$$E_{surface} = \iint \{ [\alpha_{11} w_u^2 + 2\alpha_{12} w_u w_v + \alpha_{22} w_v^2 + \beta_{11} w_{uu}^2 + 2\beta_{12} w_{uv}^2 + \beta_{22} w_{vv}^2] - 2wf(u, v) \} d_u d_v \quad (2)$$

where, w represents the obtained surface(curve) in the parameters of u, v ; w_u, w_v, w_{uu} and w_{vv} represents the first and second deviation to the direction of u, v , respectively. w_{uv} represents the deviation to u and then to v ; α, β is the given parameters; f is the given vector function; the material feature parameter is assigned to 1 and the external load is assigned to 0 under most situation.

The simplified deforming model can be represented as equation(1), which normally considers the constraints of area, length, curvature and curvature rate. The energy model can also be represented as Eq.(5) through the sum of square of curvature k_1 and k_2 .

$$E_{surface} = \iint (\alpha_{11} w_u^2 + 2\alpha_{12} w_u w_v + \alpha_{22} w_v^2 + \beta_{11} w_{uu}^2 + 2\beta_{12} w_{uv}^2 + \beta_{22} w_{vv}^2) d_u d_v \quad (3)$$

$$E_{curve} = \int k^2 d_l \quad (4)$$

$$E_{surface} = \int (k_1^2 + k_2^2) d_A \quad (5)$$

where, k - is the curvature of the required curve, k_1, k_2 is the principal curvature of the surface.

In this paper, the energy model is constructed through the physical deforming energy with boundary constraints. Once the energy function and constraints are determined, the energy surface can be solved through mathematic programming method. Here, the energy surface is represented by B-spline surface, which can optimise the repair surface through the characteristics advantages of local adjustability. The representation of B-spline surface is

$$w(u, v) = \sum_{\substack{i=0, mu \\ j=0, mv}} V_{i,j} B_{i,su}(u) B_{j,sv}(v) \quad (6)$$

where, $V_{i,j}$ is the control points of B-spline surface $w(u, v)$; $mu+1$ and $mv+1$ is the number of control points along the u, v direction, respectively; su, sv is the order of the surface on the u, v direction; $B_{i,su}(u), B_{j,sv}(v)$ is the B-spline base function along u, v direction, which is determined by su, sv order and u, v knot vector, respectively. From Eq.(6), we can get its partial derivatives on u, v variables:

$$w_u(u, v) = \sum_{\substack{i=0, mu \\ j=0, mv}} V_{i,j} B'_{i,su}(u) B_{j,sv}(v) \quad (7)$$

$$w_v(u, v) = \sum_{\substack{i=0, mu \\ j=0, mv}} V_{i,j} B_{i,su}(u) B'_{j,sv}(v) \quad (8)$$

$$w_{uu}(u, v) = \sum_{\substack{i=0, mu \\ j=0, mv}} V_{i,j} B''_{i,su}(u) B_{j,sv}(v) \quad (9)$$

$$w_{vv}(u, v) = \sum_{\substack{i=0, mu \\ j=0, mv}} V_{i,j} B_{i,su}(u) B''_{j,sv}(v) \quad (10)$$

$$w_{uv}(u, v) = \sum_{\substack{i=0, mu \\ j=0, mv}} V_{i,j} B'_{i,su}(u) B'_{j,sv}(v) \quad (11)$$

Substituting Eq.(7)~(11) into the energy model (Eq.1), and let

$$S_{i,j,k,l} = \iint \begin{bmatrix} \alpha_{11} B'_{i,su}(u) B_{j,sv}(v) B'_{k,su}(u) B_{l,sv}(v) \\ + 2\alpha_{12} B'_{i,su}(u) B_{j,sv}(v) B_{k,su}(u) B'_{l,sv}(v) \\ + \alpha_{22} B_{i,su}(u) B'_{j,sv}(v) B_{k,su}(u) B_{l,sv}(v) \\ + \beta_{11} B'_{i,su}(u) B_{j,sv}(v) B'_{k,su}(u) B_{l,sv}(v) \\ + \beta_{22} B_{i,su}(u) B'_{j,sv}(v) B_{k,su}(u) B'_{l,sv}(v) \\ + 2\beta_{12} B'_{i,su}(u) B_{j,sv}(v) B_{k,su}(u) B'_{l,sv}(v) \end{bmatrix} d_u d_v \quad (12)$$

Then, the energy model can be represented as

$$\begin{aligned}
 E &= \iint \sum_{\substack{i=0,mu \\ j=0,mv}} V_{i,j} \sum_{\substack{i=0,mu \\ j=0,mv}} V_{k,l} * S_{i,j,k,l} d_u d_v \\
 &= \sum_{\substack{i=0,mu \\ j=0,mv}} [V_{i,j} \sum_{\substack{k=0,mu \\ l=0,mv}} (V_{k,l} * S_{i,j,k,l})]
 \end{aligned} \tag{13a}$$

Or

$$E = \sum_{\substack{i=0,mu \\ j=0,mv \\ k=0,mu \\ l=0,mv}} V_{i,j} * V_{k,l} * S_{i,j,k,l} \tag{13b}$$

where, $V_{i,j}$, $V_{k,l}$ —is unknown control points; $S_{i,j,k,l}$ is a known matrix, only related with the base function of B-Spline. In the case of 3-order B-Spline, suppose that $B_{i,3}(t) = K_{(i-1)\%4}(t)$, then the matrix $S_{i,j,k,l}$ can be calculated in advance based on the B-spline base function. As a result, Eq.(13) can be transformed as a 2-order V function.

4.3. Optimal Energy Model with Boundary Constraints

Based on the energy model created above, we need to set boundary constraints expressed by control points and to solve the worn area through the method of mathematic Programming. At first, the feature points extracted from the boundary is not in a sequence, we need to rearrange these boundary points in order. Then, we divide these points into 4 sets along u,v direction which is shown in Fig.4. The number of points in u,v direction is determined automatically through a scale factor k (k=0-1) in this repair system.

For the unknown control points of the worn area which is going to be inserted, its boundary control points should be same as the control points of the boundary curve. So the solution to the unknown control points of the energy surface can be transformed into the problem of mathematic programming, which is described as follow:

$$\min E = \sum_{\substack{i=0,mu \\ j=0,mv}} \left[V_{i,j} \sum_{\substack{k=0,mu \\ l=0,mv}} (V_{k,l} * S_{i,j,k,l}) \right] \tag{14}$$

$$\text{s.t. } V_{i,0} = P_{0,i}, V_{i,mu} = P_{1,i}, \quad i = 0, 1, \dots, m_u$$

$$V_{0,j} = P_{2,j}, V_{mv,j} = P_{3,j}, \quad i = 0, 1, \dots, m_v$$

where, V represents the control point set of the whole surface, P is the feature points constraint to the boundary of the worn cavity.

Considering the linear constraints, the problem can be transformed into an optimising problem without constraints, which is represented as:

$$\min E = \sum_{\substack{i=0,mu \\ j=0,mv}} \left[V_{i,j} \sum_{\substack{k=0,mu \\ l=0,mv}} (V_{k,l} * S_{i,j,k,l}) \right] \tag{15}$$

where $V_{i,j}$ has a number of known boundary control points when $i = 0, m_u$, or $j = 0, m_v$; the other control points is unknown, which is called inner vertex to be regenerated.

To minimise the energy E of Eq.(15), we have:

$$\partial E_i / \partial V_{ij} = 0; \quad (i = 1, 2, \dots, m_u - 1; j = 1, 2, \dots, m_v - 1) \tag{16}$$

From Eq. (15) and Eq. (16), we obtain the following equations:

$$\sum_{\substack{k=0,mu&k\neq i \\ l=0,mv&l\neq j}} V_{k,l} (S_{i,j,k,l} + S_{k,l,i,j}) + 2V_{i,j} S_{i,j,i,j} = 0 \tag{17}$$

$(i = 1, 2, \dots, mu - 1; j = 1, 2, \dots, mv - 1)$

This is a $(mu - 1) \times (mv - 1)$ linear equation group, which has an equal number as the unknown control points. The problem can be solved by a number of mathematic methods. Considering the repair accuracy of the worn parts, the elimination method of Gauss principle is selected to achieve an accurate solution in this case. Once these unknown points are solved, the vertex of the cavity can be regenerated accordingly.

5. Error Evaluation

In Figure 5, there is a given surface $S(u, v)$ and a point p , we need to find a point s_c on the $S(u, v)$ which is the closest point to the point p . In other words, we need to find a point on s_c the $S(u, v)$ which has the minimum distance to the point p . As shown in Figure 5, s_{ou} and s_{ov} is point q_0 's tangent vector along u, v direction of the $S(u, v)$ surface, respectively. These two vectors construct the tangent plane Σ , the sign Π on the figure represents the projection of the direction vector $\rho = p - q_0$ on the Σ plane. According to the parallelogram rule, we have

$$\pi = s_{ou}\Delta u + s_{ov}\Delta v \tag{18}$$

where, $\Delta u, \Delta v$ represents the length of Π on the s_{ou}, s_{ov} direction, respectively. If S is a plane, q_0 can reach s_c by moving $\Delta u, \Delta v$ along u, v direction, respectively; if S is a surface, q_0 can be regarded that it has reached s_c when $|\Delta u| \leq \epsilon$ and $|\Delta v| \leq \epsilon$ is satisfied after several movements.

Based on Eq.(18), we can obtain the following express by multiplying the factor of s_{ou}, s_{ov} , respectively.

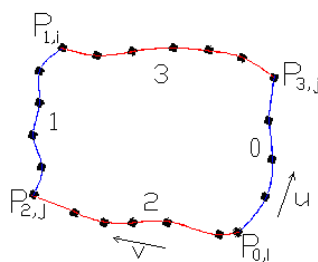


Figure 4. Boundary points divided along u, v direction

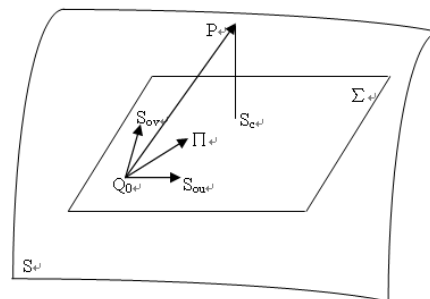


Figure 5. The closest point s_c to the point p

$$\pi \cdot s_{ou} = s_{ou}^2 \Delta u + s_{ou} s_{ov} \Delta v \tag{19}$$

$$\pi \cdot s_{ov} = s_{ou} s_{ov} \Delta u + s_{ov}^2 \Delta v \tag{20}$$

Since $\pi \cdot s_{ou} = \rho \cdot s_{ou}$, $\pi \cdot s_{ov} = \rho \cdot s_{ov}$, we can rewrite Eq.(19),Eq.(20) as below:

$$\rho \cdot s_{ou} = s_{ou}^2 \Delta u + s_{ou} s_{ov} \Delta v \quad (21)$$

$$\rho \cdot s_{ov} = s_{ou} s_{ov} \Delta u + s_{ov}^2 \Delta v \quad (22)$$

where, s_{ou} , s_{ov} is the tangent vector of point q_0 along u, v direction of the $S(u, v)$ surface, respectively. In order to get Δu , Δv , we have to solve the tangent vector s_{ou} , s_{ov} first. Below is the method to obtain the tangent vector of point q_i along u direction on the surface, which is same to the v tangent vector.

Based on the 3-order B-spline curve, we can obtain its partial deviation as follow:

$$q(u) = \sum_{j=0}^n V_j B_{j,k}(u) = \sum_{j=i-k}^i V_j B_{j,k}(u) \quad u \in [u_k, u_{n+1}] \quad (23)$$

$$q'(u) = \frac{d}{du} \left(\sum_{j=i-3}^i V_j \times B_{j,3}(u) \right) = \sum_{j=i-3}^i 3V_j \frac{B_{j,2}(u)}{u_{j+3} - u_j} - \sum_{j=i-3}^i 3V_j \frac{B_{j+1,2}(u)}{u_{j+4} - u_{j+1}} \quad (24)$$

where: V means control points of the curve, B is the base function, j is the number of B-spline, k is the order.

According to the deBoor-Cox formula, we have:

$$B_{i-3,2}(u_i) = 0, \quad \text{when } j = i - 3 \quad (25)$$

$$B_{i-2,2}(u_i) = \frac{u_{i+1} - u_i}{u_{i+1} - u_{i-1}}, \quad \text{when } j = i - 2 \quad (26)$$

$$B_{i-1,2}(u_i) = \frac{u_i - u_{i-1}}{u_{i+1} - u_{i-1}}, \quad \text{when } j = i - 1 \quad (27)$$

$$B_{i,2}(u_i) = 0, \quad \text{when } j = i \quad (28)$$

$$B_{i+1,2}(u_i) = 0, \quad \text{when } j = i + 1 \quad (29)$$

Substitute Eq. (25)~(29) into Formula (24), we can obtain the tangent vector \bar{q}'_u of q_i point along u direction:

$$q'(u) = 3(V_{i-2} - V_{i-3}) \frac{u_{i+1} - u_i}{(u_{i+1} - u_{i-2})(u_{i+1} - u_{i-1})} + 3(V_{i-1} - V_{i-2}) \frac{u_i - u_{i-1}}{(u_{i+2} - u_{i-1})(u_{i+1} - u_{i-1})}, \quad (u_i \in [u_3, u_n]) \quad (30)$$

Combining Eq. (21) and Eq. (22), we can obtain Δu , Δv . Here, we set an allowable error ε , the Convergence Criteria for the iteration will be represented as:

$$|u_{i+1} - u_i| < \varepsilon, \quad |v_{i+1} - v_i| < \varepsilon \quad (31)$$

When the criteria are not satisfied, then set $s(u_0 + \Delta u, v_0 + \Delta v)$ as the initial point, and repeat the procedure. The program iteration ends when the criteria are satisfied. The programming flowchart of the vertex error to the surface is illustrated in Fig.6..

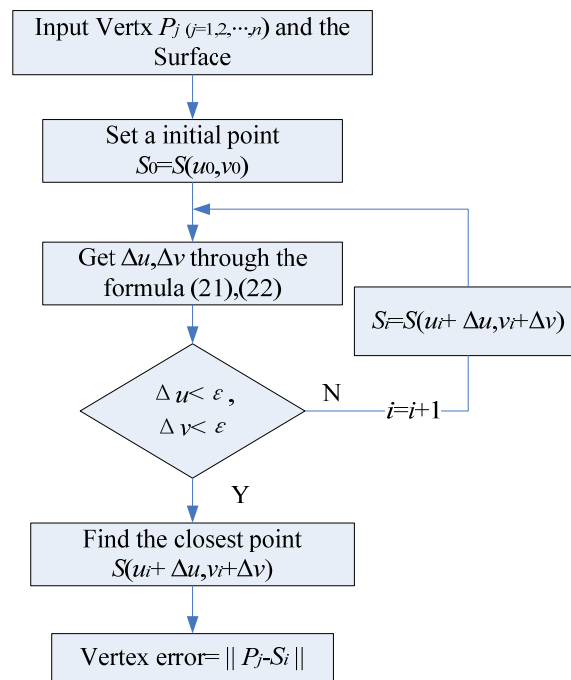


Figure 6. Flowchart of vertex error evaluation

6. Case Study

6.1. Cavity Vertex Regenerated

To demonstrate the feasibility of the method proposed, we take three examples of worn parts for this validation. Figure 7 shows the regenerated vertex for the cavity on a shaft. A number of 36 control points (4×9) is obtained from the neighbourhood of the cavity, vertex over the cavity area are regenerated which are shown in the magnified figure of Figure 7b). Figure 8 shows a model with a worn defect to be restored. In the example, the vertex of the worn area was regenerated through the approach proposed which is shown in Figure 8b). Figure 9 is another example of vertex regeneration of the proposed approach.



Figure 7. Vertex regenerated on the cavity of a shaft



Figure 8. Vertex regeneration for a worn shaft

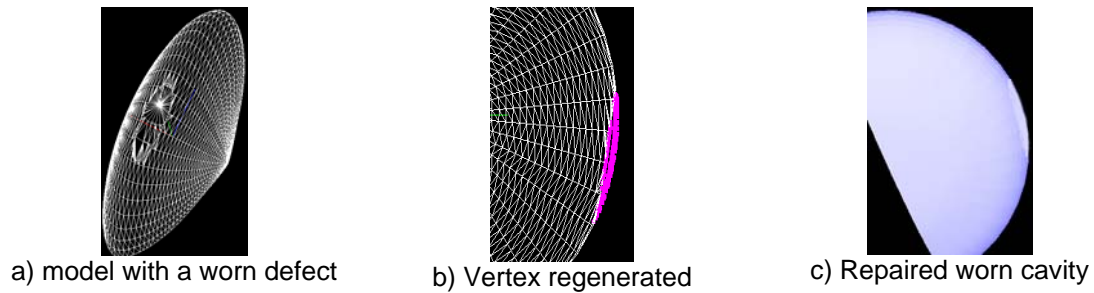


Figure 9. Vertex regenerated to the cavity on a plate part

6.2 Vertex Error Analysis

To validate the correction of the method proposed an error analysis is performed. Figure 10 (a) shows a spherical polygonal model without any defects. Through the modeling operation in Pro/E, a worn defect is added to the spherical model and a new model with the worn defect is created and inputted into the repair system for geometry reconstruction (shown in Figure 10(b)). With the method proposed, the vertex of the worn area is regenerated and shown in Figure 10(c).

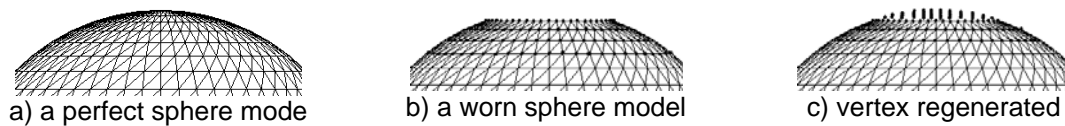


Figure 10. Vertex regeneration to a worn sphere model

For the spherical part, vertex errors can be calculated by the formula: $\delta = |op^i| - R$, where $|op^i|$ is the distance of the vertices p^i regenerated to the sphere center O, and R is the radius of the sphere. Figure 11 shows the results of vertex regenerated to the two exemplified spheres with different radius of 25mm and 18mm. In the figure, the number of regenerated vertex is marked in the sequence of the vertex creation. As the number increases the position of the vertex generated approaches to the centre of the cavity and the error increases accordingly. For the sphere of radius 25mm, the average error of the vertex on the worn area is 0.0269%, and the error STD deviation is 0.00358mm. For the sphere of radius 18mm, the average error of the vertex is 0.0157%, and the error STD deviation is 0.00124mm. Table.1 summarized the error analysis results of the two worn spheres.

Since the vertices are regenerated from the worn boundary toward the worn center, the vertex error will increase as the process approaches the center of the worn area, away from the worn boundary. Furthermore, for a large worn area, the vertex error should be bigger than that of a small worn area due to error's accumulation. As a result, the error of the vertex regenerated is small for a small worn area and it increases for large worn area.



Figure 11. Regenerated Vertices on the worn area of a sphere with R=25mm,18mm

Table1. Error comparison for the vertices regenerated

Sphere Radius R	Max Error	Min Error	Average Error(%)	STD Deviation
25mm	0.01295	0.00101	0.0269	0.00358
18mm	0.00464	0.00067	0.0157	0.00124

7. Conclusion

When complex components are worn and/or damaged, they usually are difficult or impossible to repair accurately. One of the key issues is lack of a reference model for the object to be repaired. The problem is caused by the two reasons: 1) the worn part may have a deformed geometry; 2) each component when manufactured has its own unique geometry. This paper focused on regenerating the geometry of the worn area. Based on the polygonal model of the worn part, the adjacent data on the undamaged vicinity is extracted at first. The algorithm of energy model optimization is applied to regenerate the vertices of the worn cavity. The feasibility of the proposed algorithm has been verified through several examples of worn parts. Error of the regenerated vertex is evaluated. These proposed methods are implemented in a repair system through Visual C++6.0 program. Once the vertices of the worn area are regenerated, they can be used for surface reconstruction and further for the tool path generation for build up and machining processes. Further research work will be carried out on improving the accuracy and efficiency of the regeneration method, especially, for repairing of damaged parts with large worn area.

Acknowledgments

This project is sponsored by the National Natural Foundation of China (Grant No. 51175093), by the Specialized Research Fund for the Doctoral Program of Higher Education of China (Grant No. 20094420110001) and by Guangdong Provincial Science and Technology R&D Project (Grant No. 2009B010900048, No. 2010B090400458, No. 2010A080401003).

References

- [1] Gao J, Gindy N, and Chen X. Automated GD&T Inspection System based on Non-contact 3D Digitisation. *International Journal of Production Research*. 2006; 44 (1): 117-134.
- [2] Gao J, Chen X, Yilmaz O and Gindy N. An integrated adaptive repair solution for complex aerospace components through geometry reconstruction. *The International Journal of Advanced Manufacturing Technology*. 2008; 36(11-12): 1170-1179
- [3] Bagci E. Reverse engineering applications for recovery and re-manufacturing: Three case studies. *Advances in Engineering Software*. 2009; 40: 407-418.
- [4] Automated repair and overhaul of aero-engine components, *Engine Yearbook*. 2005; 80-83.
- [5] Walton P. Adaptive machining shows its mettle in manufacture and repair, <http://www.ttl-3d.co.uk/>. Accessed on 5 September 2003.
- [6] Dix B. Aerofoil machining and polishing combined into a single automated process. *International Journal: Aircraft Engineering and Aerospace Technology*. 2004; 76(5).
- [7] Yilmaz O, Gindy N, and Gao J. A study of turbomachinery components machining and repairing methodologies. *Aircraft Engineering and Aerospace Technology: An International Journal*. 2005; 77(6): 455-466.
- [8] Huang J. Research on Explicit Algorithm of Local Interpolation and its application, PhD Thesis, Macao University of Science and Technology; 2005.
- [9] Gao J, Chen X, Zheng DT, Yilmaz O and Gindy NNZ. Adaptive Restoration of Complex Geometry Parts through Reverse Engineering Application. *Advances in Engineering Software*. 2006; 37(9): 592-600
- [10] Stiller J. Point-normal interpolation schemes reproducing spheres cylinders and cones. *Geometric Design*. 2007; 24(5): 286-301.
- [11] Peters J. Local smooth surface interpolation: a classification. *Computer Aided Geometric Design*. 1990; 7(1-4): 191-195.
- [12] Wang YB, Sheng YH, Lv GN, et al. A Delaunay-based Surface Reconstruction Algorithm for Unorganized Sampling Points. *Journal of Image and Graphics*. 2007; 12(9): 1537-1543.
- [13] Li JG, Yang D, Meng XH, et al. Conforming Voronoi Tessellation in 3D. *Journal of Computer-Aided Design & Computer Graphics*. 2005; 17(10): 2143-2151.

- [14] Zhang XY, Zhang SY, Ye XZ. "Interactive free-form deformation for sculpture". *Journal of Computer-Aided Design & Computer Graphics*. 2005; 17(11): 2420-2426.
- [15] Miller JV, Breen DE, Lorensen WE, et al. Geometrically deformed models: a method for extracting closed geometric models from volume data. *SIGGRAPH'91*. 1991; 25(4): 217-226.
- [16] Gu P, Yan X. Neural network approach to reconstruction of freeform surfaces for reverse engineering. *Computer Aided Design*. 1995; 27(1): 59-64.
- [17] Wang HT, Zhang LY, Li ZW, et al, B-spline surface reconstruction from scattered data points based on SOM neural network, *Journal of Image and Graphics*. 2007; 12(2): 349-355.
- [18] Zhang LW, Hu TB, Liu XL, et al. *Surface Reconstruction from Cloud Points Based on Support Vector Machine*, Proceedings of the IEEE International Conference on Automation and Logistics, Qingdao, China September 2008; PP377-381.
- [19] Cai Y, Xiao J. Surface reconstruction from points based on support vector machine. *Journal of System Simulation*. 2007; 19(15): 2027-2029.
- [20] Chui C, Lai MJ. Filling polygonal holes using C1 cubic triangular spline patches. *Computer Aided Geometric Design*. 2000; 17: 297-307.
- [21] Curless B, Levoy M. A volumetric method for building complex models from range image. *Comput Graphics (Proc SIGGRAPH)*. 1996; 303-12.
- [22] Liepa P. Filling holes in meshes. *Eurographics Symposium on Geometric Processing*. 2003; 200-7.
- [23] Jun Y. A piecewise hole filling algorithm in reverse engineering. *Computer-Aided Design*. 2005; 37: 263-270.
- [24] Wang JN, Oliveira MM. Filling holes on locally smooth surfaces reconstructed from point clouds. *Image and Vision Computing*. 2007; 25: 103-113.
- [25] Bardell R, Balendran V, and Sivayoganathan K. Accuracy analysis of 3D data collection and free-form modelling methods. *Journal of Materials Processing Technology*. 2003; 133: 26-33.
- [26] Chen LC, and Lin GC. Reverse Engineering in the design of turbine blades - a case study in apply the MAMDP. *Robotics and Computer Integrated Manufacturing*. 2000; 16: 161-167.
- [27] Motavalli S, Review of Reverse Engineering Approaches. *Computers & Industrial Engineering*. 1998; 35(1-2): 25-28.
- [28] Zhang SJ, Raja VH, Fernandes KJ, et al. Rapid prototyping models and their quality evaluation using reverse engineering. *Proc. Instn. Mech. Eng., Part B: J. Eng Manuf*. 2003; 217(Special issue): 81-96.
- [29] Werner A, Skalski K, Piszczatowski S, et al. Reverse engineering of free-form surfaces. *Journal of Materials Processing Technology*. 1998; 76: 128-132.
- [30] Gao J, Ma ZX, Chen X, and Zheng DT, *Polygonal Model based Vertex Regeneration Method for Refurbishment of Worn Parts*. Proceedings of the 17th CIRP International Conference on Life Cycle Engineering, LCE2010; 19-21 May 2010. Hefei, China.